

Received Date : 28-Jun-2016
Revised Date : 04-Oct-2016
Accepted Date : 06-Oct-2016
Article type : Research Report

Comparative effects of adaptation on layer II-III and layer V-VI neurons in cat V1

**Nayan Chanauria^a, Vishal Bharmauria^{a,b}, Lyes Bachatene^{a,c}, Sarah Cattan^a,
Jean Rouat^{a,c}, Stéphane Molotchnikoff^a**

^a Neurophysiology of Visual System, Département de Sciences Biologiques, Université de Montréal, CP 6128 Succursale Centre-Ville, Montréal, QC, Canada, H3C 3J7

^b The Visuomotor Neuroscience Lab, Centre for Vision Research, Faculty of Health, York University, 4700 Keele Street, Toronto, Ontario, M3J 1P3

^c Department of Nuclear Medicine and Radiobiology, Faculty of Medicine and Health Sciences (CHUS), SNAIL | Sherbrooke Neuro Analysis and Imaging Lab, University of Sherbrooke, Quebec, J1K 2R1

^d Département de Génie Électrique et Génie Informatique, Université de Sherbrooke, Sherbrooke, QC, Canada

Corresponding author details

Dr. Stéphane Molotchnikoff

Professor

Dept. Sciences Biologiques

Université de Montreal

CP 6128 Succ Centre-Ville

Montreal, QC, H3C 3J7, Canada

stephane.molotchnikoff@umontreal.ca

This article has been accepted for publication and undergone full peer review but has not been through the copyediting, typesetting, pagination and proofreading process, which may lead to differences between this version and the Version of Record. Please cite this article as doi: 10.1111/ejn.13439

This article is protected by copyright. All rights reserved.

Abstract:

V1 is fundamentally grouped into columns that descend from layer II-III to layer V-VI. Neurons inherent to visual cortex are capable of adapting to changes in the incoming stimuli that drive the cortical plasticity. A principle feature called orientation selectivity can be altered by the presentation of non-optimal stimulus called 'adapter'. When triggered, LGN cells impinge upon layer IV and further relay the information to deeper layers via layer II-III. Using different adaptation protocols, neuronal plasticity can be investigated. Superficial neurons in area V1 are well acknowledged to exhibit attraction and repulsion by shifting their tuning peaks when challenged by a non-optimal stimulus called 'adapter'. Layer V-VI neurons in spite of partnering layer II-III neurons in cortical computation, have not been explored simultaneously towards adaptation. We believe that adaptation not only affects cells specific to a layer but modifies the entire column. In this study, through simultaneous multiunit recordings in anesthetized cats using a multichannel depth electrode, we show for the first time how layer V-VI neurons (1000-1200 μm) along with layer II-III neurons (300-500 μm) exhibit plasticity in response to adaptation. Our results demonstrate that superficial and deeper layer neurons react synonymously towards adapter by exhibiting similar behavioral properties. The neurons displayed similar amplitude of shift and maintained equivalent sharpness of Gaussian tuning peaks before and the following adaptation. It appears that a similar mechanism, belonging to all layers, is responsible for the analogous outcome of the neurons' experience with adapter.

Introduction

Neuroplasticity refers to the brain's ability to reorganize itself as a result of experience. It was previously thought that neuroplasticity declines with aging, but it is now well established that neurons in the mature brain can alter their properties, too (Holtmaat & Svoboda, 2009). Several experiments using specific protocols (such as visual deprivation, environmental enriching, and adaptation) have demonstrated that neurons can modify their properties well into adulthood. Visual adaptation has been the approach to understanding the phenomenon of plasticity and we continue to uncover new findings in different regions of the brain.

Visual cortex (V1) is the classical model to study neuronal plasticity. V1 cortices of higher mammals are organized into domains of preferred selectivity known as orientation columns. Neuronal orientation selectivity can be altered by imposing a non-optimal stimulus (adapter) within receptive fields of neurons for a certain period of time (Dragoi *et al.*, 2000; Kohn, 2007; Ghisovan *et al.*, 2009; Nemri *et al.*, 2009; Bachatene *et al.*, 2012; Cattani *et al.*,

2014). Contingent upon the stimulus duration, neurons change their orientation selectivity either towards or away from the adapter, exhibiting attractive or repulsive shifts, respectively (Dragoi *et al.*, 2000; Kohn, 2007; Jeyabalaratnam *et al.*, 2013). Shorter adaptation durations (< 3 min) largely produce repulsive shifts (Dragoi *et al.*, 2000), whereas longer duration adaptation (up to 12 min) imparts attractive shifts (Dragoi *et al.*, 2000; Ghisovan *et al.*, 2009; Bachatene *et al.*, 2012; Jeyabalaratnam *et al.*, 2013; Cattani *et al.*, 2014).

An orientation column is divided into supragranular or upper layers (layer I and II-III), the central granular layer (layer IV), and infragranular or lower layers (layers V and VI). Neurons in a column are highly similar with respect to stimulus properties such as orientation, direction, speed, contrast, spatial frequency, etc. (Hubel *et al.*, 1977; Blasdel & Salama, 1986). Conventionally, information is received by layer IV neurons from the lateral geniculate nucleus (LGN), processed in the supragranular layers of the visual cortex, and then projected on to infragranular neurons. Interestingly, recently investigators (Agmon & Connors, 1992; Meyer *et al.*, 2010; Wimmer *et al.*, 2010; Oberlaender *et al.*, 2012; Constantinople & Bruno, 2013; Rah *et al.*, 2013; Pluta *et al.*, 2015) have shown that deeper cortical layers receive direct thalamic input that activates infragranular neurons. This suggests that layer IV is not necessarily the only port of information flow to other cortical layers.

Historically, numerous studies have investigated the effects of adaptation on layer II-III neurons (Dragoi *et al.*, 2000; Bachatene *et al.*, 2013; Jeyabalaratnam *et al.*, 2013; Cattani *et al.*, 2014; Bachatene *et al.*, 2015). One of these reports (Dragoi *et al.*, 2000) has shown that neurons recorded between 500-1500 μm of cortical depth also display a shift in orientation tuning in response to the adapter. Yet, no report has simultaneously explored the effects of adaptation on layers II-III and V-VI neurons. Since the cortical column extends from layer II-III to layer V-VI, and because of extensive connectivity (Helmstaedter *et al.*, 2009; Jiang *et al.*, 2013; DeNardo *et al.*, 2015; Lee *et al.*, 2015) between supra- and infragranular neurons, we hypothesize that effect of adaptation is not confined to specific

layer of the cortex but it prevails throughout the column, subsequently gained by neurons of adjacent columns, leading to whole cortex reprogramming. Therefore, it is of interest to simultaneously examine the effects of adaptation on both layers II-III and V-VI.

We used anesthetized cats to investigate the effects of adaptation on simultaneously recorded supra- and infragranular layer neurons using a multichannel depth electrode in V1 at 300-500 μm and 1000-1200 μm from the surface. We found that layer II-III and V-VI neurons exhibited comparable attractive and repulsive shifts with no significant differences in the average shift-amplitudes and orientation selectivity. In line with our recent findings (Bachatene *et al.*, 2015) and the results of the current investigation, we suggest that supra- and infragranular layer neurons change their selectivity in parallel in response to adaptation which possibly explains that supra- and infragranular neurons interact with each other in a column. This study also points toward specific feedforward and feedback loops between supra- and infragranular neurons that may be responsible for robust functional reprogramming of orientation columns in V1 (Bachatene *et al.*, 2015).

Materials and methods

Ethical approval

Electrophysiological recordings were performed in the area17 of six adult domestic cats (*Felis catus*) of either sex. The animal surgery procedure and electrophysiological recordings were performed according to the guidelines of the Canadian Council on Animal Care and were approved by the Institutional Animal Care and Use Committee of the University of Montreal. Animals were supplied by the Division of Animal Resources of the University of Montreal. Experiments were carried out in accordance with the guidelines approved by the NIH in the USA, the Canadian Council on Animal Care, and the Institutional Animal Care and Use Committee of University of Montreal (CDEA) regarding the care and use of animals for experimental procedures.

Anaesthesia

Cats were first sedated with acepromazine maleate [1 mg/kg, intramuscular (i.m.), Atravet; Wyeth-Ayerst, Guelph, Ontario, Canada] and atropine sulfate (0.04 mg/kg, i.m., Atrosa; Rafter, Calgary, Alberta, Canada), and anesthetized with ketamine hydrochloride (25 mg/kg, i.m., Rogarsetic; Pfizer, Kirkland, Quebec, Canada). Anesthesia was maintained during the surgery with isoflurane ventilation (2%, AErrane; Baxter, Toronto, Ontario, Canada). After the surgery, cats were paralyzed by perfusion of gallamine tri ethiodide (40 mg/kg, intravenous, Flaxedil; Sigma Chemical, St Louis, MO, USA), fixed in a stereotaxic apparatus, and artificially ventilated with O₂/N₂O (30:70) mixture containing isoflurane (0.5%). Paralysis was maintained by perfusion of gallamine tri ethiodide (10 mg/kg per h) in 5% dextrose lactated Ringer's nutritive solution throughout the experiment.

Surgery

Lidocaine hydrochloride (Xylocaine, AstraZeneca, Mississauga, ON, Canada; 2%) was injected subcutaneously as a local anesthetic during the surgery. A tracheotomy was performed for artificial ventilation, and one forelimb vein was cannulated. Before fixing the animals on the stereotaxic apparatus, xylocaine gel (Astra Pharma, Mississauga, ON, Canada; 5%) was applied on the pressure points to reduce pain and sensation. Proper depth of anesthesia was ensured throughout the experiment by monitoring the EEG, the electrocardiogram, and the expired CO₂. The end-tidal CO₂ partial pressure was kept constant between 25 and 30 mmHg. A heated pad was placed beneath the cat to maintain a body temperature of 37.5°C. Tribissen (Schering-Plough, PointeClaire, QC, Canada; 30 mg kg⁻¹ per day, subcutaneous) and Duplocillin (Intervet, Withby, ON, Canada; 0.1 ml kg⁻¹, intramuscular) were administered to the animals to prevent bacterial infection. A craniotomy (1×1 cm) was performed over the primary visual cortex (area 17/18, Horsley-Clarke coordinates P0–P6; L0–L6). The underlying dura was removed, and the depth electrode was

positioned in area 17. The pupils were dilated with atropine sulfate (Isopto-Atropine, Alcon, Mississauga, ON, Canada; 1%) and the nictitating membranes were retracted with phenylephrine hydrochloride (Mydrin, Alcon, Mississauga, ON, Canada; 2.5%). Plano contact lenses with artificial pupils (5 mm diameter) were placed on the cat's eyes to prevent the cornea from drying (University of Montreal, PQ, Canada). At the end of each experiment, the cats were euthanized with a lethal dose of pentobarbital sodium (Somnotol, MTC Pharmaceuticals, Cambridge, ON, Canada; 100 mg kg⁻¹) by an intravenous injection.

Visual stimulation

Stimulation was performed monocularly. After clearly detectable activity was obtained, the multiunit receptive fields (RF) were mapped by using a hand-held ophthalmoscope (Barlow *et al.*, 1967). Receptive field edges were determined by moving a light bar from the periphery towards the center until a response was evoked. Visual stimuli were generated with a VSG 2/5 graphic board (Cambridge Research Systems, Rochester, England) and displayed on a 21 inch Monitor (Sony GDM-F520 Trinitron, Tokyo, Japan) placed 57 cm from the cat's eyes, with 1024x768 pixels, running at 100 Hz frame refresh. This is schematized in Figure 1A. Stimuli were drifting sine-wave gratings covering the excitatory RF (Maffei *et al.*, 1973). The receptive fields were located centrally within a 15° radius from the fovea. Contrast and mean luminance were set at 80% and 40 cd/m² respectively. Optimal spatial and temporal frequencies were set at 0.24 cycles/deg and in the range 1.0–2.0 Hz (at these values V1 neurons are driven maximally) by sine-wave drifting gratings (Bardy *et al.*, 2006).

Electrophysiological recording

Multi-unit activity in the primary visual cortex was recorded using a tungsten multichannel depth electrode (0.1- 0.8 M Ω at 1 KHz; Alpha Omega Co. USA Inc.) (Figure 1A, right). The recordings were performed in both hemispheres of the cat's brain. The electrode consisted of four micro-electrodes in a linear array (inter-electrode spacing 500 μ m) enclosed in stainless steel tubing. The signal from the microelectrodes was amplified, band-pass filtered (300 Hz – 3 KHz), digitized and recorded with a 0.05 ms temporal resolution (Spike2, CED, Cambridge, UK). We recorded at average cortical depths of 300-500 μ m and 1000-1200 μ m simultaneously from both sites. To further confirm the location of contacting electrodes, histological staining and local field potentials (LFP's) were recorded for every site where the electrode tip was lowered. Figure 1B (left) shows a histological section of area 17 and confirms the location of the electrode at the appropriate depth. Further, LFPs were recorded (low-pass filtered between 10 -100 Hz) to observe the sink-source dipoles. To evoke LFP's, a series of drifting gratings oriented at 0° to 157.5° separated by 22.5° was presented (each oriented flash lasted 100 ms) covering the whole screen of the monitor. Figure 1B (right) displays the LFP traces of layer II-III and layer V-VI neurons. The inversion of polarity (positive-negative LFP, red arrows) at both electrodes further validates the correct positioning of electrodes.

The multiunit activity of neurons was recorded simultaneously from layer II-III and layer V-VI. Figure 1C (right) shows an example of neuronal isolation (spike sorting) from the multiunit activity. Spike sorting was done offline using Spike2 package, CED, Cambridge, England. The single units were discriminated based upon the spike waveforms, principal component analysis (PCA) and auto correlograms (ACG). The respective PCA, ACGs, and spike-waveforms are shown to the right (Figure 1C).

Adaptation Protocol

After manually mapping the receptive fields, eight different orientations were presented randomly one-by-one within the receptive fields of the neurons. Eight oriented sine wave drifting gratings were presented in a random order ranging from 0° to 157.5° at regular intervals of 22.5°. Each orientation was presented in a block of 25 trials (each trial lasted 4.1 s) with varying inter-stimulus (1–3 s) intervals during which no stimulus was presented. Thus, the presentation of one oriented drifting grating lasted ~180 s (including all trials and inter-stimulus intervals) (Figure 1A). Once the control orientation tuning curves were characterized, an adapting oriented stimulus (non-optimal orientation) was presented continuously for 12 min (Figure 1A) within the receptive fields of neurons. The adapting stimulus was a drifting grating whose orientation was chosen based on the multiunit activity values obtained at control conditions and was generally set within 22.5° to 67.5° of the neurons' preferred orientations. No recordings were performed during this adaptation period. Immediately after the adaptation procedure, recordings were performed starting with the adaptor orientation and initially preferred orientation followed by recording of remaining orientations in a random fashion. Finally, the tuning curves were computed as below.

Data

The Gaussian tuning fits were computed for neurons pre- and post-adaptation using the function below:

$$y = y_0 + \left(A \div \left(w \times \sqrt{\frac{\pi}{2}} \right) \right) \times e^{-2 \times \left(\frac{x - x_c}{w} \right)^2}$$

where y_0 is the offset, x_c is the center, w is the width and A represents the area under the Gaussian fit. The firing rates were normalized in Prism and Gaussian tuning curves were generated in the scientific software Origin. The direction and magnitude of shifts were

calculated as the distance between peak positions of the fitted Gaussian tuning curves before and after adaptation (the difference between the initially preferred and newly acquired). An attractive shift was attributed to the displacement peak of the orientation tuning curve in the direction of the adapter while a repulsive shift was indicated by a displacement of the tuning peak in opposite direction (away from the adapter). As indicated in the methods these displacements should be $>5^\circ$ to be considered as a significant shift.

Moreover, we also measured the orientation selectivity index (OSI) of a neuron by dividing the firing rate at the orthogonal orientation by the firing rate at the preferred orientation, and subtracting the result from 1 (Ramoa *et al.*, 2001; Liao *et al.*, 2004; Bachatene *et al.*, 2013). The closer the OSI is to 1, the stronger the orientation selectivity. Finally, the sorted neurons were classified into regular and fast spikes on the basis of the spike-width (Bartho *et al.*, 2004; Schwindel *et al.*, 2014; Bharmauria *et al.*, 2015). Spikes with a width < 0.3 ms were identified as fast spiking neurons (FS) and > 0.3 ms as regular spiking (RS) neurons.

Statistical tests

Three data sets were tested for statistics: 1) amplitudes of shift (attractive and repulsive) values 2) OSI values of neurons pre- and post-adaptation 3) spike width values. These data were tested for normal distribution using the D'Agostino & Pearson omnibus normality test. Based on the results obtained, parametric student t-test (unpaired) was applied to the values of shift amplitudes. Further, all four groups (attractive shift values in layer II-III and layer V and repulsive shift values in layer II-III and layer V) were compared with ANOVA. On the other hand, non-parametric Mann-Whitney test was employed to the values of OSI and spike width of neurons since these distributions were not normal. The Pearson coefficient was calculated to find any correlation between the data groups. To infer the difference in proportions z-test was used. Consequently, comparisons were drawn between attractive and repulsive populations and spike width values obtained for either layer. Finally, a regression

analysis was done to find correlation between spike width values and amplitude of attractive and repulsive shifts.

Results

The goal of the current investigation was to explore the effect of adaptation on simultaneously recorded neurons from supra- and infragranular layers. In total, 97 neurons were recorded and analyzed for the effects of 12 min adaptation on each layer. A comparative post-adaptation behavioral distribution of cells in either layer is shown in Figure 2. The gray shades and green shades represent the supra- and infragranular layers respectively. The color scheme is respected throughout the manuscript. In fact, neurons in both layers exhibited similar shift tendencies. The graph on the upper right shows the proportion of cells showing attractive and repulsive shifts. On comparing the proportion of attractive shifts between the two layers, infragranular neurons exhibited a higher proportion ($p = 0.05$, t-test) of attractive shifts as compared to supragranular neurons. However, this is not the case for repulsive shifts ($p = 0.70394$, t-test).

A part of the remaining population refracted the adapter and did not show any significant shift ($<5^\circ$) in orientation tuning (Bachatene *et al.*, 2013; Jeyabalaratnam *et al.*, 2013; Bachatene *et al.*, 2015). The corresponding proportion of repulsive shifts for both layers were found to be comparable (06 neurons in supra- and 07 in infragranular layers). A fraction of tuned (T) neurons lost their selectivity post-adaptation and was categorized as T-U (17 in supra- and 20 in infragranular layers). Moreover, some untuned (U) neurons acquired novel selectivity after adaptation and were categorized as U-T (20 neurons in supra- and 09 in infragranular layers). A proportion analysis was not performed on these latter data sets since we were primarily interested in comparing only attractive and repulsive behaviors across layers. Such novel selectivity has been reported previously in mice (Jeyabalaratnam *et al.*, 2013). It is to be underlined that neurons with an orientation

selectivity index (OSI) < 0.5 were classified as untuned (Bharmauria *et al.*, 2015; Bharmauria *et al.*, 2016). Finally, a minority of neurons (09 in supra- and 05 in infragranular layers) remained untuned before and after adaptation (U to U).

Layer II-III and layer V-VI primary visual neurons co-ordinate to acquire a novel preference

The effects of adaptation have been extensively studied in layer II-III neurons (Dragoi *et al.*, 2000; Bachatene *et al.*, 2013; Jeyabalaratnam *et al.*, 2013; Cattan *et al.*, 2014; Bachatene *et al.*, 2015). Because a column extends from layer II-III to layer V-VI it was of interest to investigate the effects of adaptation on simultaneously recorded neurons from both layers. Thus, we examined the post-adaptation orientation tuning curves of simultaneously recorded layer II-III and layer V-VI neurons. Figure 3 shows typical examples of adaptation effects (shifts in orientation selectivity) on both layers after 12 minutes of adaptation. In Figure 3A, an example of each type of effect (attractive, repulsive, and no shift) is shown for layer II-III. The top and middle rows show the raw tuning curves of neurons pre- and post-adaptation. The superimposed Gaussian fits are shown at the bottom demonstrating the shifts. To the left, an attractive shift is illustrated. In the control condition, the neuron was optimally tuned to 158.47° (OSI = 0.9; $R^2 = 0.6$). After adapting the neuron for 12 minutes with a 45° grating (red arrow), the selectivity of the neuron (OSI = 0.9; $R^2 = 0.5$) shifted toward the adapter (57.34°), that is, the neuron exhibited an attractive shift. The middle column shows an example of a repulsive shift. The neuron in this case changed its preference away from 91.24° (OSI = 0.9; $R^2 = 0.8$) to 30.77° (OSI = 0.9; $R^2 = 0.6$) after being challenged with 112° adapter. Similarly, the third column (extreme right) illustrates an example of a refractory neuron. This neuron did not change its preference after adaptation with 45° grating and maintained its selectivity at approximately 67° . The selectivity minutely changed from 67.1°

(OSI = 0.8; $R^2 = 0.5$) to 68.22° orientation (OSI = 0.8; $R^2 = 0.8$) and it was deemed non-significant.

In a similar fashion, the results are demonstrated in Figure 3B for layer V-VI neurons. To the left, a typical example of an attractive shift is illustrated. The neuron was originally selective to 52.61° orientation (OSI = 0.9; $R^2 = 0.7$) but acquired a novel optimal selectivity of 136.54° (OSI = 0.8; $R^2 = 0.5$) after 12 minutes of adaptation with 90°. The middle column represents an example of a repulsive shift. Here, the layer V-VI neuron was optimally tuned to 39.57° orientation (OSI = 0.8; $R^2 = 0.6$). After imposing the 22.5° adapter the neuron changed its preference away from the adapter to 72.30° orientation (OSI = 0.9; $R^2 = 0.6$) showing a repulsive shift. Finally, on the right, a refractory neuron is displayed. This neuron, in spite of being adapted with 45° adapter, did not change its preference. It maintained its preference around 74° and changed its selectivity non-significantly from 74.2° (OSI = 0.7; $R^2 = 0.9$) to 73.4° (OSI = 0.9; $R^2 = 0.9$).

Further, the amplitudes of attractive and repulsive shifts were plotted to compare the magnitude of orientation shift in layer II-III and layer V-VI neurons (Figure 4A). The difference in mean (\pm SEM) amplitude of attractive shifts for layer II-III (mean = 49.68 ± 4.37) and layer V-VI neurons (42.23 ± 3.77) was found not significant (t-test, $p = 0.1030$). A similar result was found for the amplitude of repulsive shifts (mean \pm SEM) 33.06 ± 3.96 and 32.88 ± 5.18 for layers II-III and V-VI respectively (t-test, $p = 0.9778$). However, attractive shifts (Att = 49.67 ± 4.36 ; Rep = 33.06 ± 3.958) in layer II-III were found dominant over repulsive shifts ($p = 0.0056$). Moreover, on comparing all four groups (one-way ANOVA, $p = 0.0361$) the mean difference was found to be significant. This could be indicative of individual cells in both layers behaving independently yet following a similar trend globally.

In addition, Orientation Selectivity Index (OSI) was also computed for all the neurons in layers II-III and V-VI to investigate the tuning sharpness of neurons before and after adaptation. Figure 4B shows the mean of OSI for 97 neurons each for layer II-III and V-VI at control and post-adaptation conditions. The mean (mean \pm SEM) OSI for neurons at control and post-adaptation conditions was found to be 0.65 ± 0.03 and 0.60 ± 0.03 (Mann-Whitney test, $p = 0.7863$) for layer II-III neurons and 0.65 ± 0.03 and 0.65 ± 0.02 (Mann-Whitney test, $p = 0.2446$) for layer V-VI neurons, respectively. The difference in mean OSI was not significant in both layers which further indicate that neurons in layer II-III and V-VI acquire the new selectivity in an analogous mode, thus maintaining the homeostasis post-adaptation. These results also support the fact that, following adaptation, the orientation columns (extending from layer II-III to layer V-VI) tilt in such a fashion that the functional dogma of columns is maintained as shown previously (Bachatene *et al.*, 2015). To summarize, following adaptation the cellular dynamics in a column remain unchanged which reflects that the 'entire block' of cells is displaced after being challenged by the adapter.

Relation between the spike-width and amplitude of shift

Neurons were dissociated into broad/regular spiking (RS) and narrow/fast spiking neurons (FS) on the basis of their spike width (Bharmauria *et al.*, 2015; Bharmauria *et al.*, 2016). The RS and FS neurons have been putatively linked to excitatory and inhibitory neurons (Nowak *et al.*, 2003; Niell & Stryker, 2008; Vinck *et al.*, 2013). It was reported that a large population of excitatory neurons in cats' visual cortex exhibit narrow spike shape, consequently not permitting a clear distinction between pyramidal and inhibitory cells (Nowak *et al.*, 2003). Nevertheless, in the current study, a spike-width threshold of 0.3 ms was chosen to separate the neurons (Bharmauria *et al.*, 2015; Bharmauria *et al.*, 2016) (Figure 5). Figure 5A illustrates separated neurons. Neurons having spike width > 0.3 ms were categorized into RS neurons, whereas neurons exhibiting a spike width ≤ 0.3 ms were classified into FS

neurons. The division was performed separately for both layers. The inserts of spike waveforms on the right side of figure 5A (gray and green) illustrate how the classification was done. Layer V neurons showed a wide range of spike width in comparison to layer II-III. However, on averaging the values of spike widths for different groups, the values were found comparable in both layers. The proportion of RS and FS cells were found no different from each other as evident from figure 5C (shows the proportion of RS and FS cells). The z-test for proportion was performed for both layers (p -value = 0.50926). To see the global pattern of RS and FS groups in either layer, mean \pm SEM of RS and FS neurons was calculated (Figure 5B). The mean values were found to be 0.47 ± 0.01 and 0.24 ± 0.01 for layer II-III and 0.48 ± 0.01 and 0.24 ± 0.006 for layer V-VI respectively. For this data, a non-parametric Mann-Whitney test was employed. The p -values for RS and FS data were found to be 0.5084 and 0.5155, respectively.

Additionally, a sub-categorisation was performed to compare the direction of shift with the type of cell. This was done to compare shift trends in RS and FS neurons (Figure 6). We found layer II-III (mean \pm SEM = 52.60 ± 4.65) and layer V-VI (mean \pm SEM = 45.96 ± 4.80) RS neurons shifting towards the attractive direction with the largest amplitude (t-test, $p = 0.3271$). This tendency of RS neurons was also observed in the repulsive direction but with a lesser magnitude. The means (mean \pm SEM) of the amplitude of repulsive shifts in layer II-III and layer V-VI RS neurons were found comparable (t-test, $p = 0.6181$) and their values were found to be 32.88 ± 7.64 and 33.70 ± 4.78 , respectively. Moreover, layer II-III FS (attractive = 40 ± 7.32 ; repulsive = 33.20 ± 4.11) and V-VI FS (attractive = 34.46 ± 5.54 ; repulsive = 31.50 ± 12.05) neurons also exhibited shifts in attractive ($p = 0.6181$) and repulsive ($p = 0.8747$) directions showing comparable values of means. The proportion of neurons showing attractive and repulsive shifts (Figure 6, insert on the upper right) were computed which showed that FS neurons in layer V shift more towards the adapter i.e. in the attractive direction in comparison to layer II-III neurons. Lastly, neurons exhibiting no shifts were also included in the graph but no significance was observed between groups. This indicated that

overall, in supra- and infragranular layers both RS and FS neurons showcase attractive and repulsive shifts and with a similar tendency of shifts post-adaptation.

To further see a correlation between spike width values and amplitude of shifts a regression analysis for either layer was done between spike width values and amplitude of shift (Figure 7). None of the four groups showed a relation between compared values. Thus, all above analyses seem to indicate that cells within a column operate in a uniform fashion implying that cells of the entire cortical column from superficial to deep layers change their properties towards imposed non-preferred orientation following adaptation. However, it is important to note that individual cells could play different and specific roles in achieving an equilibrium state.

To the best of our knowledge, this is the first comparative study of the simultaneously recorded layer II-III and layer V-VI neurons in adult cat V1 in response to adaptation that shows an overall picture of events occurring in an orientation column following adaptation.

Discussion

In summary, we demonstrated that layer II-III and layer V-VI neurons acquired comparable orientation selectivity shifts after 12 minutes of adaptation. The main results of the current investigation are: 1) in addition to the layers II-III, layer V-VI neurons also exhibit orientation selectivity shifts; 2) the mean amplitudes of attractive and repulsive shifts in both layers are comparable; 3) the average OSI pre- and post-adaptation in either layer is similar, and; 4) the mean amplitude of shifts of RS and FS neurons in both layers is about equal. These results are in line with the previous findings by (Bachatene *et al.*, 2015) who showed that neurons in supragranular layers reprogram their orientation selectivity when adapted visually and this reprogramming is so systematic that neurons even in the non-adapted columns

acquire the new selectivity with respect to the previous column which seems to be guided by the adapting column.

Layer II-III neurons exhibit attractive and repulsive shifts (Ghisovan & Nemri, 2008; Ghisovan *et al.*, 2009; Nemri *et al.*, 2009; Bachatene *et al.*, 2012). In the present investigation, we show for the first time that infragranular layer V-VI neurons also show these classical shifts in orientation selectivity in conjunction with layer II-III neurons in response to adaptation.

Generally, neurons recorded from an electrode tip shift their orientation selectivity in a similar direction. In other words, this small pool of neurons recorded from the same tip is affected by an identical mechanism in response to the external stimulus called 'adapter' (Nemri *et al.*, 2009). A previous study based on adaptation (Dragoi *et al.*, 2000) showed that neuronal shifts are independent of cortical depth. Anatomical evidence suggests that neurons sharing orientation preference are mostly connected with each other and are present in the orientation domains whereas neurons situated close to pinwheels are connected with neurons having a wide range of orientation preference (Schummers *et al.*, 2004, Maldonado *et al.*, 1997). The present investigation is based on electrophysiological recordings, however, the fact that locations of neurons in the orientation map can affect several of their inherent features, e.g., shift amplitude, the direction of shift, etc., can't be ignored. It would be inequitable to compare individual populations recorded from different regions of the orientation map. Hence, this study focuses more towards the global response pattern of supra- and infragranular neurons and not on response behavior of an individual neuron. Nevertheless, when the sub- populations are examined deeply, different properties are displayed by individual cells, e.g., some clusters (recording from a single site down the column) are homogeneous showing attractive shifts whereas others are heterogeneous displaying attraction and repulsion. This is one of the possible reasons for a large variance of the shift amplitudes and it explains why neurons in either layer display a large range of orientation shift amplitude.

The orientation selectivity index (OSI) which is calculated by the sharpness of the tuning curve of a neuron was also calculated for both layers at control and post-adaptation conditions. The OSI was comparable for layer V-VI and layer II-III neurons confirming the neurons maintained an optimal tuning prior to and post-adaptation.

Next, the neurons were classified into RS and FS cells putatively referred to as excitatory and inhibitory neurons, respectively, throughout the literature (Povysheva *et al.*, 2006; Fries *et al.*, 2007; Gouwens *et al.*, 2010; Hofer *et al.*, 2011). Firstly, we observed both groups of cells showing attractive and repulsive shifts. It indicated that shift in orientation selectivity is independent of V1 neuron type. Secondly, we also found fast spiking neurons exhibiting a repulsive shift of smaller magnitude as compared to regular spiking neurons exhibiting attractive shifts. Similar results were confirmed previously (Bachatene *et al.*, 2012) for supragranular layer II-III neurons. Lastly, we found equal proportions of putative excitatory and inhibitory neurons in our data which suggested that the regular and fast spiking neurons exist in balance across cortical layers.

To further infer a relation between the type of neuron and the direction of shift we sub-categorised RS and FS neurons into three groups: cells showing attractive shifts, repulsive shifts, and no shift (Bachatene *et al.*, 2012). The observation revealed that RS neurons shift with a higher magnitude than fast spiking neurons in both layers. This is indeed indicative of RS neurons being more plastic than FS neurons. Another important observation was made about fast spiking neurons. Layer II-III FS neurons were found more likely to shift in a repulsive direction rather than attractive direction and this pattern was reversed in the layer V. It could also be indicative of a possible specific role of inhibitory neurons in the adaptation process. A recent review (Naka *et al.*, 2016) discussed several types of inhibitory neurons in layer V that play specific roles in different types of inhibition mechanisms particularly in layer V. Layer II-III neurons form the densest projection on layer V neurons and synaptically recruit them to fire. This generates a robust feed-forward inhibition. Connectivity studies in different regions of the brain suggest that this feed-forward inhibition

between layer II-III and layer V neurons is unique as different layer V neurons receive different strengths of excitatory inputs from layer II-III neurons (Pouille et al., 2009; Adesnik and Scanziani, 2010; Jin et al., 2014; Pluta et al., 2015; Jiang et al., 2015; Otsuka and Kawaguchi, 2009). Layer V is not only an output layer but also an important input layer as it receives inputs from all other cortical layers (Markram et al., 2015). Therefore, it is worth noting the role of inhibitory neurons specifically in layer V. This could potentially form another possible explanation of how neurons across layers behave differently yet they maintain equilibrium inside the orientation column.

Adaptation Mechanism:

The underlying mechanism of adaptation may involve transient changes at the synapse level occurring at different time scales dependent on the duration of adaptation (Kohn, 2007).

Adaptation mainly involves a decrease in the response to the initially preferred orientation and increasing the response towards the dominant orientation. This decrease in the firing rate generally occurs at the individual level and could be a consequence of a change in membrane properties of V1 cells, e.g., hyperpolarisation (Carandini & Ferster, 1997) or synaptic depression or slow hyperpolarising of Na⁺ channels (Sanchez-Vives et al., 2000).

Inhibition and excitation play a major role in creating and maintaining the equilibrium by recurrently modulating the response gain in local cortical circuits (Ben-Yishai et al., 1995; Douglas et al., 1995; Somers et al., 1995). Other disinhibitory mechanisms may also be critical to maintaining homeostasis during the adaptation process.

Possible functional implications:

It has been amply demonstrated and suggested that a neuron's single dendritic branch receives synaptic inputs from differently tuned neurons. This enables the neuron to be able to elicit a response to a wide range of inputs by making synaptic associations. The dominant input then drives the corresponding synapses giving rise to an optimal selectivity for the neuron (Jia *et al.*, 2010; Bachatene *et al.*, 2013; Wertz *et al.*, 2015) Within this framework, the imposition of an adapter grating strengthens the synapses related to it, thus potentiating a novel selectivity for the neuron. Thus, a new adjustment between the excitation and inhibition after the adaptation period facilitates the neurons to acquire a new selectivity.

A possible explanation is that repulsion is a consequence of a default reaction. Following adaptation, the "new" preferred orientation acquired by the same neuron is an outcome of a differential decrease in response to the initially preferred orientation, while flank orientations far from the adapter in the tuning curve remain relatively unchanged. However, the latter orientations evoke a stronger response and became dominant. Therefore, attractive shifts are the outcome of dual modulation of responses, a push-pull mechanism that simultaneously diminishes responses to the original preferred orientation and increases firing to orientations close to the adapter. Consequently, the final data obtained is the product of modifications of ratios between excitatory and inhibitory inputs. Since similar results are observed in supra- and infragranular layers, it is reasonable to conclude that in both layers excitatory and inhibitory populations share similar mechanisms (Kohn & Movshon, 2004; Ghisovan *et al.*, 2009). Moreover, the excitatory and inhibitory loops may also be implicated in this robust recalibration of neuronal selectivity (Froemke, 2015).

In the passage of neuronal information in the visual cortex, layer IV neurons are the receiving units of the information coming from the thalamus (LGN), and these neurons project the information to layer II-III neurons. Further, the information is conveyed to infragranular layer V-VI neurons (Kapfer *et al.*, 2007; Otsuka & Kawaguchi, 2009; Apicella *et*

al., 2012; Jiang *et al.*, 2015). In addition, several studies demonstrate that there are abundant anatomical connections between layer II-III and V-VI neurons (Lowenstein & Somogyi, 1991; Thomson & Bannister, 2003). However, it has also been shown that infragranular layers receive a direct input from the thalamic cells (Constantinople & Bruno, 2013; Pluta *et al.*, 2015). These interneuronal relationships may be the basis for shifts in these layers occurring through a common mechanism(s).

The co-active groups of neurons are termed as microcircuits or cell assemblies (Buzsaki, 2010; Harris & Mrsic-Flogel, 2013; Singer, 2013; Bharmauria *et al.*, 2014; Miller *et al.*, 2014; Bharmauria *et al.*, 2015). The behavior of individual neurons in these assemblies is dependent on inputs from neighboring or distally located neurons horizontally or as a function of depth. The dynamics of the synapses induce a change in the orientation tuning of neurons during the process of training layer II-III and layer V-VI neurons together. Therefore, goal-directed functional synaptic communications configure the underlying mechanisms for the neurons to change their tuning across different layers (Felsen *et al.*, 2002). Moreover, shifts in orientation selectivity are credited to the short-term plasticity of intra-cortical connections. Therefore, these interactions between synapses of neighboring neurons (horizontally or as a function of depth) support the plasticity in the brain (Harvey & Svoboda, 2007).

Collectively, we observed that cortical layer V-VI and layer II-III neurons show similar responses to adaptation which suggests that neurons in supragranular and infragranular layers strive in alliance with each other, suggesting that neurons not specific to a layer respond to adaptation distinctively, but the whole V1 column changes leading to a whole cortex re-orientation. Considering the cortical column as a functional unit of the visual cortex, it appears that neurons in a column choose to perform in unison to propagate a comprehensive harmony in the cortical column which is preserved from column to column and, as a consequence of training one of the columns, the whole cortex is recalibrated towards maintaining that balance to achieve its stable state.

References:

Adesnik, H. & Scanziani, M. (2010). Lateral competition for cortical space by layer-specific horizontal circuits. *Nature*, **464**, 1155-1160.

Agmon, A. & Connors, B. (1992) Correlation between intrinsic firing patterns and thalamocortical synaptic responses of neurons in mouse barrel cortex. *J. Neurosci.*, **12**, 319-329.

Apicella, A. J., Wickersham, I. R., Seung, H. S. & Shepherd, G. M. G. (2012) Laminarly orthogonal excitation of fast-spiking and low-threshold-spiking interneurons in mouse motor cortex. *J. Neurosci.*, **32**, 7021-7033.

Bachatene, L., Bharmauria, V., Cattan, S. & Molotchnikoff, S. (2013) Fluoxetine and serotonin facilitate attractive-adaptation-induced orientation plasticity in adult cat visual cortex. *Eur. J. Neurosci.*, **38**, 2065-2077.

Bachatene, L., Bharmauria, V., Cattan, S., Rouat, J. & Molotchnikoff, S. (2015) Reprogramming of orientation columns in visual cortex: a domino effect. *Sci. Reports*, **5**, 9436.

Bachatene, L., Bharmauria, V., Rouat, J. & Molotchnikoff, S. (2012) Adaptation-induced plasticity and spike waveforms in cat visual cortex. *Neuroreport*, **23**, 88-92.

Bardy, C., Huang, J.Y., Wang, C., FitzGibbon, T. & Dreher, B. (2006) 'Simplification' of responses of complex cells in cat striate cortex: suppressive surrounds and 'feedback' inactivation. *J. Physiol.*, **574**, 731-750.

Barlow, H.B., Blakemore, C. & Pettigrew, J.D. (1967) The neural mechanism of binocular depth discrimination. *J. Physiol.*, **193**, 327-342.

Bartho, P., Hirase, H., Monconduit, L., Zugaro, M., Harris, K.D. & Buzsaki, G. (2004) Characterization of neocortical principal cells and interneurons by network interactions and extracellular features. *J. Neurophysiol.*, **92**, 600-608.

Ben-Yishai, R., Bar-Or, R. L., Sompolinsky, H. (1995). Theory of orientation tuning in visual cortex. *Proc. Natl. Acad. Sci. USA*, **9**, 3844-8.

Bharmauria, V., Bachatene, L., Cattan, S., Brodeur, S., Chauria, N., Rouat, J. & Molotchnikoff, S. (2016) Network-selectivity and stimulus - discrimination in the primary visual cortex: cell-assembly dynamics. *Eur. J. Neurosci.*, **43**, 204-219.

Bharmauria, V., Bachatene, L., Cattan, S., Chauria, N., Rouat, J. & Molotchnikoff, S. (2015) Stimulus-dependent augmented gamma oscillatory activity between the functionally connected cortical neurons in the primary visual cortex. *Eur. J. Neurosci.*, **41**, 1587-1596.

Bharmauria, V., Bachatene, L., Cattan, S., Rouat, J. & Molotchnikoff, S. (2014) Synergistic activity between primary visual neurons. *Neuroscience*, **268**, 255-264.

Blasdel, G.G. & Salama, G. (1986) Voltage-sensitive dyes reveal a modular organization in monkey striate cortex. *Nature*, **321**, 579-585.

Buzsaki, G. (2010) Neural syntax: cell assemblies, synapsembles, and readers. *Neuron*, **68**, 362-385.

Carandini, M. & Ferster, D (1997). A tonic hyperpolarization underlying contrast adaptation in cat visual cortex. *Science*, **276**, 949-52.

Cattan, S., Bachatene, L., Bharmauria, V., Jeyabalaratnam, J., Milleret, C. & Molotchnikoff, S. (2014) Comparative analysis of orientation maps in areas 17 and 18 of the cat primary visual cortex following adaptation. *Eur. J. Neurosci.*, **40**, 2554-2563.

Constantinople, C.M. & Bruno, R.M. (2013) Deep cortical layers are activated directly by thalamus. *Science*, **340**, 1591-1594.

DeNardo, L.A., Berns, D.S., DeLoach, K. & Luo, L. (2015) Connectivity of mouse somatosensory and prefrontal cortex examined with trans-synaptic tracing. *Nat. Neurosci.*, **18**, 1687-1697.

Douglas, R.J., Koch, C. Mahowald, M., Martin, K.A., Suarez, H.H. (1995). Recurrent excitation in neocortical circuits. *Science*, **269**, 981-5.

Dragoi, V., Sharma, J. & Sur, M. (2000) Adaptation-induced plasticity of orientation tuning in adult visual cortex. *Neuron*, **28**, 287-298.

Felsen, G., Shen, Y.S., Yao, H., Spor, G., Li, C. & Dan, Y. (2002) Dynamic modification of cortical orientation tuning mediated by recurrent connections. *Neuron*, **36**, 945-954.

Fries, P., Nikolic, D. & Singer, W. (2007) The gamma cycle. *Trends Neurosci.*, **30**, 309-316.

Froemke, R.C. (2015) Plasticity of cortical excitatory-inhibitory balance. *Ann. Rev. Neurosci.*, **38**, 195-219.

Ghisovan, N. & Nemri, A. (2008) How fast can we adapt? *J. Physiol.*, **586**, 1213-1214.

Ghisovan, N., Nemri, A., Shumikhina, S. & Molotchnikoff, S. (2009) Long adaptation reveals mostly attractive shifts of orientation tuning in cat primary visual cortex. *Neuroscience*, **164**, 1274-1283.

Gouwens, N.W., Zeberg, H., Tsumoto, K., Tateno, T., Aihara, K. & Robinson, H.P. (2010) Synchronization of firing in cortical fast-spiking interneurons at gamma frequencies: a phase-resetting analysis. *PLoS Comput. Biol.*, **6**, e1000951.

Harris, K.D. & Mrsic-Flogel, T.D. (2013) Cortical connectivity and sensory coding. *Nature*, **503**, 51-58.

Harvey, C.D. & Svoboda, K. (2007) Locally dynamic synaptic learning rules in pyramidal neuron dendrites. *Nature*, **450**, 1195-1200.

Helmstaedter, M., Sakmann, B. & Feldmeyer, D. (2009) Neuronal correlates of local, lateral, and translaminar inhibition with reference to cortical columns. *Cereb. Cortex*, **19**, 926-937.

Hofer, S.B., Ko, H., Pichler, B., Vogelstein, J., Ros, H., Zeng, H., Lein, E., Lesica, N.A. & Mrsic-Flogel, T.D. (2011) Differential connectivity and response dynamics of excitatory and inhibitory neurons in visual cortex. *Nat. Neurosci.*, **14**, 1045-1052.

Holtmaat, A. & Svoboda, K. (2009) Experience-dependent structural synaptic plasticity in the mammalian brain. *Nat. Rev. Neurosci.*, **10**, 647-658.

Hubel, D.H., Wiesel, T.N. & LeVay, S. (1977) Plasticity of ocular dominance columns in monkey striate cortex. *Philosophical transactions of the Royal Society of London. Series B, Biological sciences*, **278**, 377-409.

Jeyabalaratnam, J., Bharmauria, V., Bachatene, L., Cattan, S., Angers, A. & Molotchnikoff, S. (2013) Adaptation shifts preferred orientation of tuning curve in the mouse visual cortex. *PLoS One*, **8**, e64294.

Jia, H., Rochefort, N.L., Chen, X. & Konnerth, A. (2010) Dendritic organization of sensory input to cortical neurons in vivo. *Nature*, **464**, 1307-1312.

Jin, X., Jiang, K., and Prince, D.A. (2014). Excitatory and inhibitory synaptic connectivity to layer V fast-spiking interneurons in the freeze lesion model of cortical microgyria. *J. Neurophysiol.*, **122**, 1703–1713.

Jiang, X., Shen, S., Cadwell, C.R., Berens, P., Sinz, F., Ecker, A.S., Patel, S. & Tolias, A.S. (2015) Principles of connectivity among morphologically defined cell types in adult neocortex. *Science*, **350**, aac9462.

Jiang, X., Wang, G., Lee, A.J., Stornetta, R.L. & Zhu, J.J. (2013) The organization of two new cortical interneuronal circuits. *Nat. Neurosci.*, **16**, 210-218.

Kapfer, C., Glickfeld, L.L., Atallah, B.V. & Scanziani, M. (2007) Supralinear increase of recurrent inhibition during sparse activity in the somatosensory cortex. *Nat. Neurosci.*, **10**, 743-753.

Kohn, A. (2007) Visual adaptation: physiology, mechanisms, and functional benefits. *J. Neurophysiol.*, **97**, 3155-3164.

Kohn, A. & Movshon, J.A. (2004) Adaptation changes the direction tuning of macaque MT neurons. *Nat. Neurosci.*, **7**, 764-772.

Lee, A.J., Wang, G., Jiang, X., Johnson, S.M., Hoang, E.T., Lanté, F., Stornetta, R.L., Beenhakker, M.P., Shen, Y. & Julius Zhu, J. (2015) Canonical organization of layer 1 neuron-led cortical inhibitory and disinhibitory interneuronal circuits. *Cereb. Cortex*, **25**, 2114-2126.

Liao, D.S., Krahe, T.E., Prusky, G.T., Medina, A.E. & Ramoa, A.S. (2004) Recovery of cortical binocularity and orientation selectivity after the critical period for ocular dominance plasticity. *J. Neurophysiol.*, **92**, 2113-2121.

Lowenstein, P.R. & Somogyi, P. (1991) Synaptic organization of cortico - cortical connections from the primary visual cortex to the posteromedial lateral suprasylvian visual area in the cat. *J. Comparat. Neurol.*, **310**, 253-266.

Maldonado, P. E., Godecke, I., Gray, C. M., Bonhoeffer, T. (1997). Orientation selectivity in pinwheel centers in cat striate cortex. *Science*, **276**, 1551-5.

Maffei, L., Fiorentini, A. & Bisti, S. (1973) Neural correlate of perceptual adaptation to gratings. *Science*, **182**, 1036-1038.

Markram, H., Muller, E., Ramaswamy, S., Reimann, M.W., Abdellah, M., Sanchez, C.A., et al. (2015). Reconstruction and simulation of neocortical microcircuitry. *Cell*, **163**, 456–492.

Meyer, H.S., Wimmer, V.C., Hemberger, M., Bruno, R.M., de Kock, C.P.J., Frick, A., Sakmann, B. & Helmstaedter, M. (2010) Cell type-specific thalamic innervation in a column of rat vibrissa cortex. *Cereb. Cortex*, **20**, 2287-2303.

Miller, J.E., Ayzenshtat, I., Carrillo-Reid, L. & Yuste, R. (2014) Visual stimuli recruit intrinsically generated cortical ensembles. *Proc. Natl. Acad. Sci. USA*, **111**, E4053-4061.

Naka, A. & Adesnik, H. (2016). Inhibitory circuits in cortical layer 5. *Front. Neural Circuits*, **10**, 35.

Nemri, A., Ghisovan, N., Shumikhina, S. & Molotchnikoff, S. (2009) Adaptive behavior of neighboring neurons during adaptation-induced plasticity of orientation tuning in VI. *BMC Neurosci.*, **10**, 147.

Niell, C.M. & Stryker, M.P. (2008) Highly selective receptive fields in mouse visual cortex. *J. Neurosci.*, **28**, 7520-7536.

Nowak, L.G., Azouz, R., Sanchez-Vives, M.V., Gray, C.M. & McCormick, D.A. (2003) Electrophysiological classes of cat primary visual cortical neurons in vivo as revealed by quantitative analyses. *J. Neurophysiol.*, **89**, 1541-1566.

Oberlaender, M., de Kock, C.P.J., Bruno, R.M., Ramirez, A., Meyer, H.S., Dercksen, V.J., Helmstaedter, M. & Sakmann, B. (2012) Cell type-specific three-dimensional structure of thalamocortical circuits in a column of rat vibrissal cortex. *Cereb. Cortex*, **22**, 2375-2391.

Otsuka, T. & Kawaguchi, Y. (2009) Cortical inhibitory cell types differentially form intralaminar and interlaminar subnetworks with excitatory neurons. *J. Neurosci.*, **29**, 10533-10540.

Otsuka, T., & Kawaguchi, Y. (2013). Common excitatory synaptic inputs to electrically connected cortical fast-spiking cell networks. *J. Neurophysiol.* **110**, 795–806.

Pluta, S., Naka, A., Veit, J., Telian, G., Yao, L., Hakim, R., Taylor, D. & Adesnik, H. (2015) A direct translaminar inhibitory circuit tunes cortical output. *Nat. Neurosci.*, **18**, 1631-1640.

Pouille, F., Marin-Burgin, A., Adesnik, H., Atallah, B.V., and Scanziani, M (2009). Input normalization by global feedforward inhibition expands cortical dynamic range. *Nat. Neurosci.*, **12**, 1577–1585.

Povysheva, N.V., Gonzalez-Burgos, G., Zaitsev, A.V., Kroner, S., Barrionuevo, G., Lewis, D.A. & Krimer, L.S. (2006) Properties of excitatory synaptic responses in fast-spiking interneurons and pyramidal cells from monkey and rat prefrontal cortex. *Cereb. Cortex*, **16**, 541-552.

Rah, J.-C., Bas, E., Colonell, J., Mishchenko, Y., Karsh, B., Fetter, R.D., Myers, E.W., Chklovskii, D.B., Svoboda, K., Harris, T.D. & Isaac, J.T.R. (2013) Thalamocortical input onto layer 5 pyramidal neurons measured using quantitative large-scale array tomography. *Front. Neural Circuits*, **7**, 177.

Ramoá, A.S., Mower, A.F., Liao, D. & Jafri, S.I. (2001) Suppression of cortical NMDA receptor function prevents development of orientation selectivity in the primary visual cortex. *J. Neurosci.*, **21**, 4299-4309.

Sanchez-Vives, M. V., Nowak, L. G., McCormick, D. A. (2000). Cellular mechanisms of long-lasting adaptation in visual cortical neurons in vitro. *J. Neurosci.*, **11**, 4286-99.

Schummers, J., Marino, J., Sur, M. (2004). Local networks in visual cortex and their influence on neuronal responses and dynamics. *J. Physiol. Paris*, **98**, 429-41.

Schwindel, C.D., Ali, K., McNaughton, B.L. & Tatsuno, M. (2014) Long-term recordings improve the detection of weak excitatory-excitatory connections in rat prefrontal cortex. *J. Neurosci.*, **34**, 5454-5467.

Singer, W. (2013) Cortical dynamics revisited. *Trends Cognit. Sci.*, **17**, 616-626.

Somers, D. C., Nelson, S. B., Sur, M. (1995). An emergent model of orientation selectivity in cat visual cortical simple cells. *J. Neurosci.*, **15**, 5448-5465.

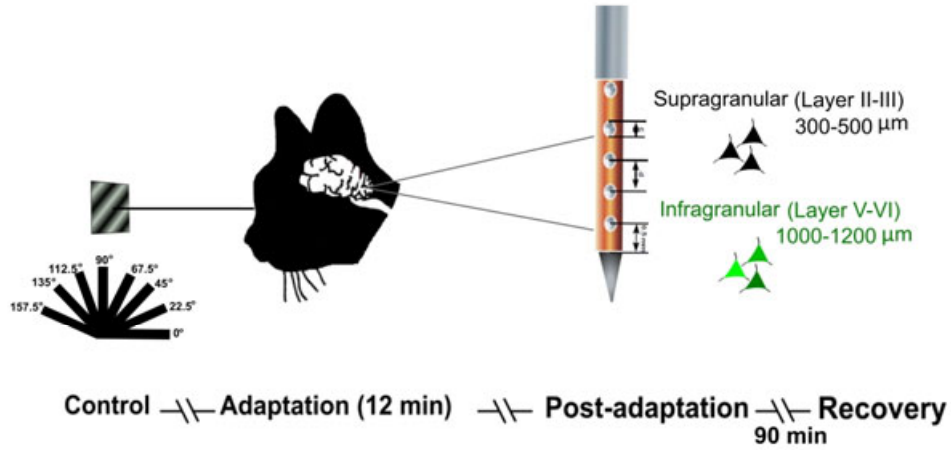
Thomson, A.M. & Bannister, A.P. (2003) Interlaminar Connections in the Neocortex. *Cereb. Cortex*, **13**, 5-14.

Vinck, M., Womelsdorf, T., Buffalo, E.A., Desimone, R. & Fries, P. (2013) Attentional modulation of cell-class-specific gamma-band synchronization in awake monkey area v4. *Neuron*, **80**, 1077-1089.

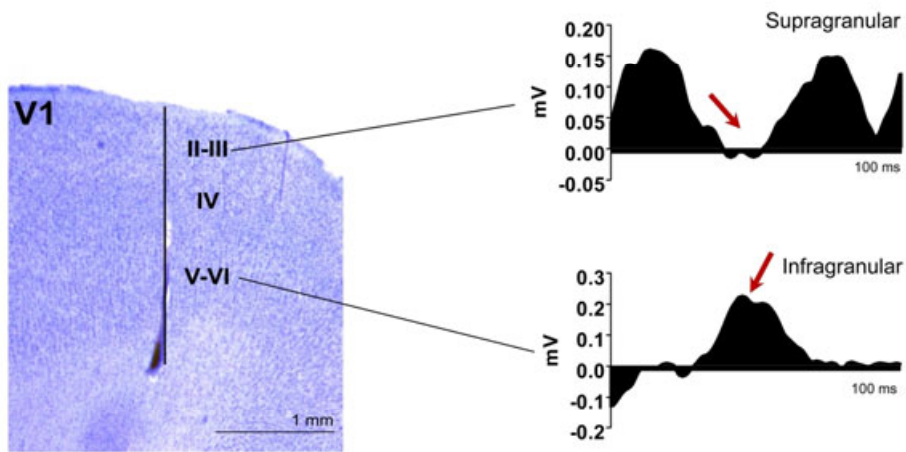
Wertz, A., Trenholm, S., Yonehara, K., Hillier, D., Raics, Z., Leinweber, M., Szalay, G., Ghanem, A., Keller, G., Rozsa, B., Conzelmann, K.K. & Roska, B. (2015) PRESYNAPTIC NETWORKS. Single-cell-initiated monosynaptic tracing reveals layer-specific cortical network modules. *Science*, **349**, 70-74.

Wimmer, V.C., Bruno, R.M., de Kock, C.P.J., Kuner, T. & Sakmann, B. (2010) Dimensions of a Projection Column and Architecture of VPM and POM Axons in Rat Vibrissal Cortex. *Cereb. Cortex*, **20**, 2265-2276.

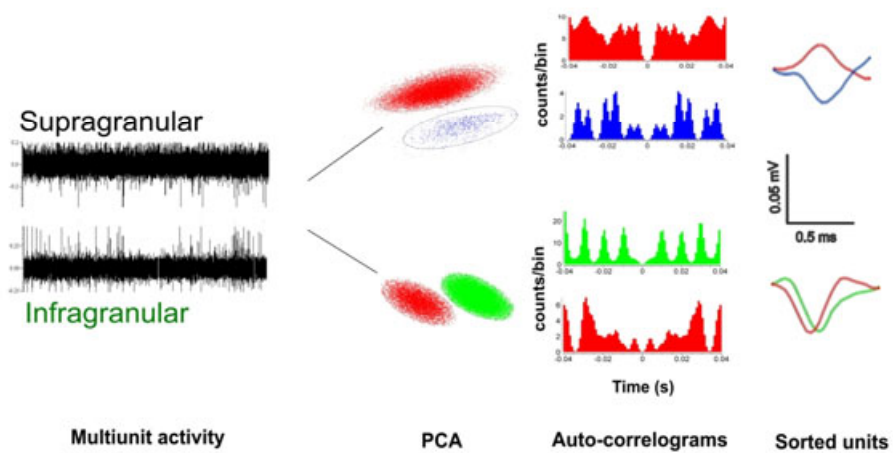
A

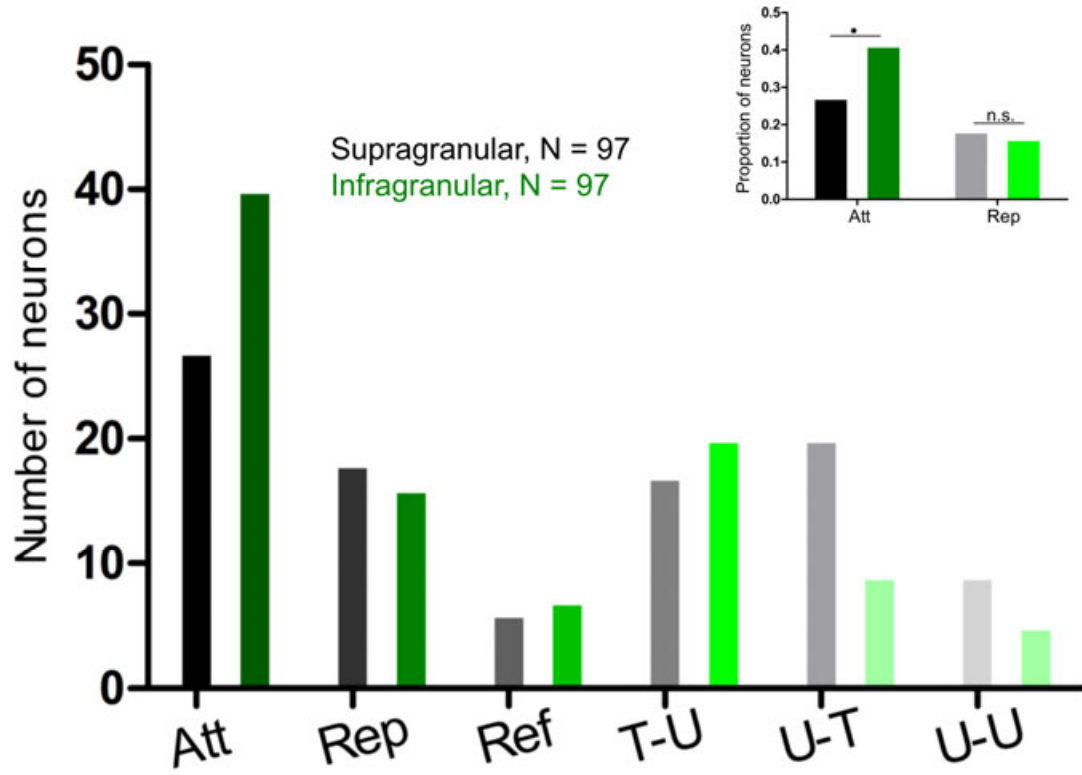


B

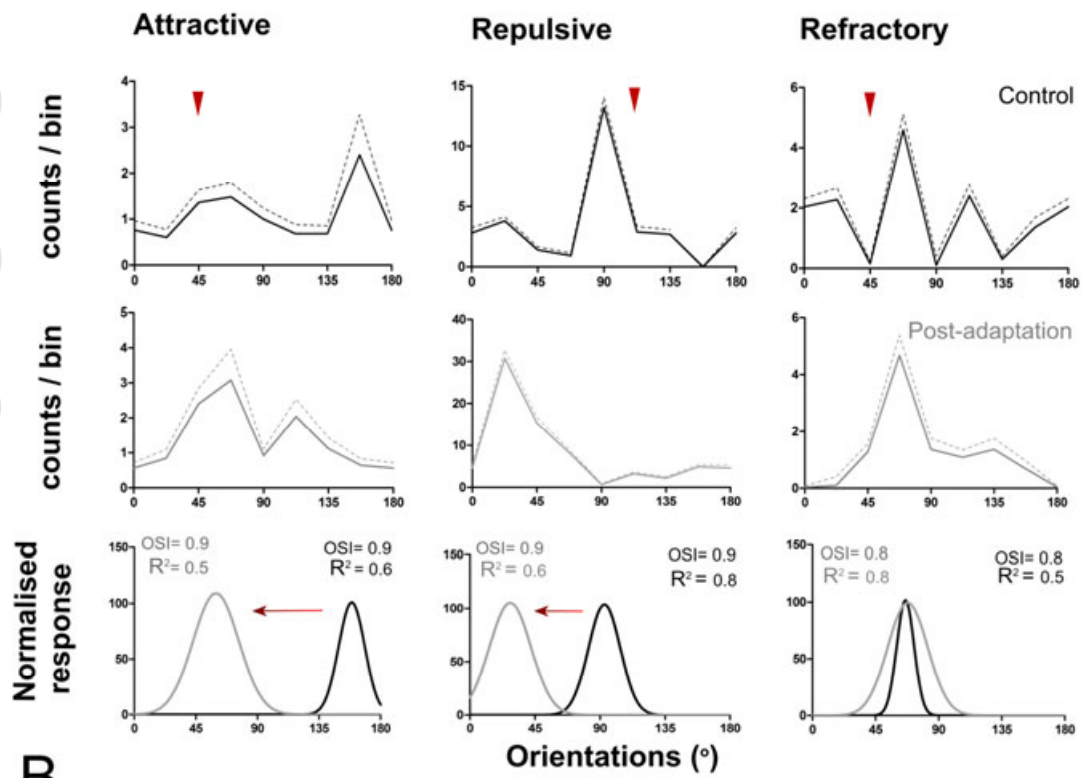


C

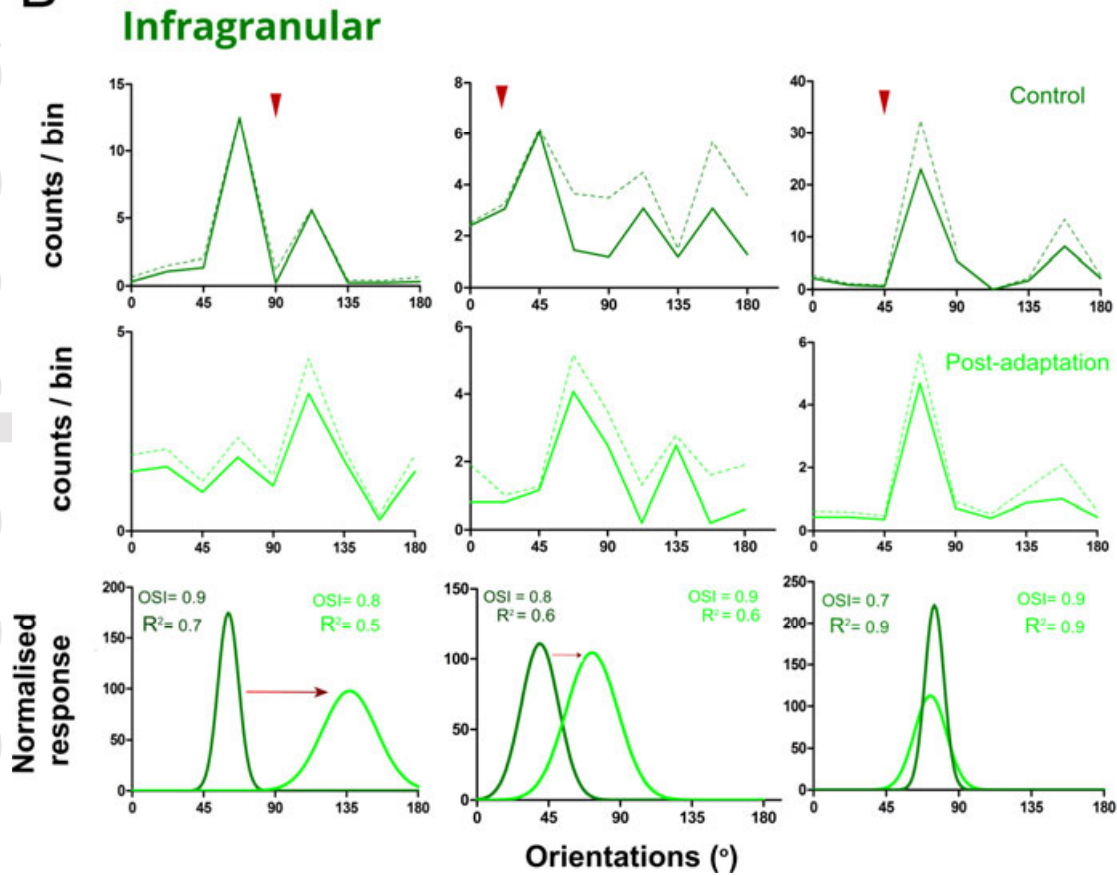


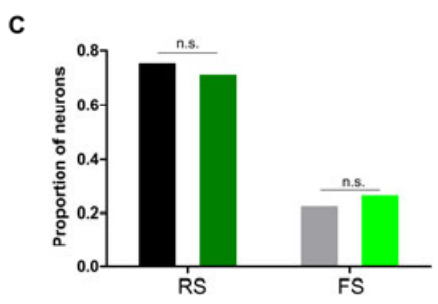
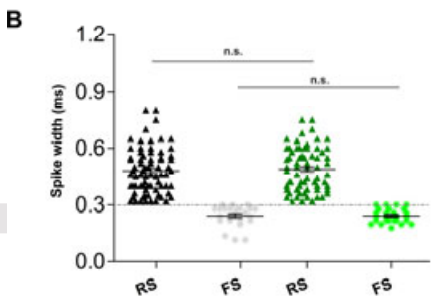
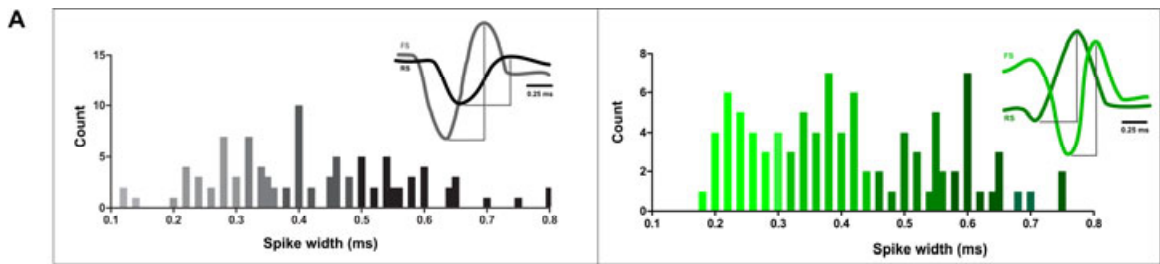
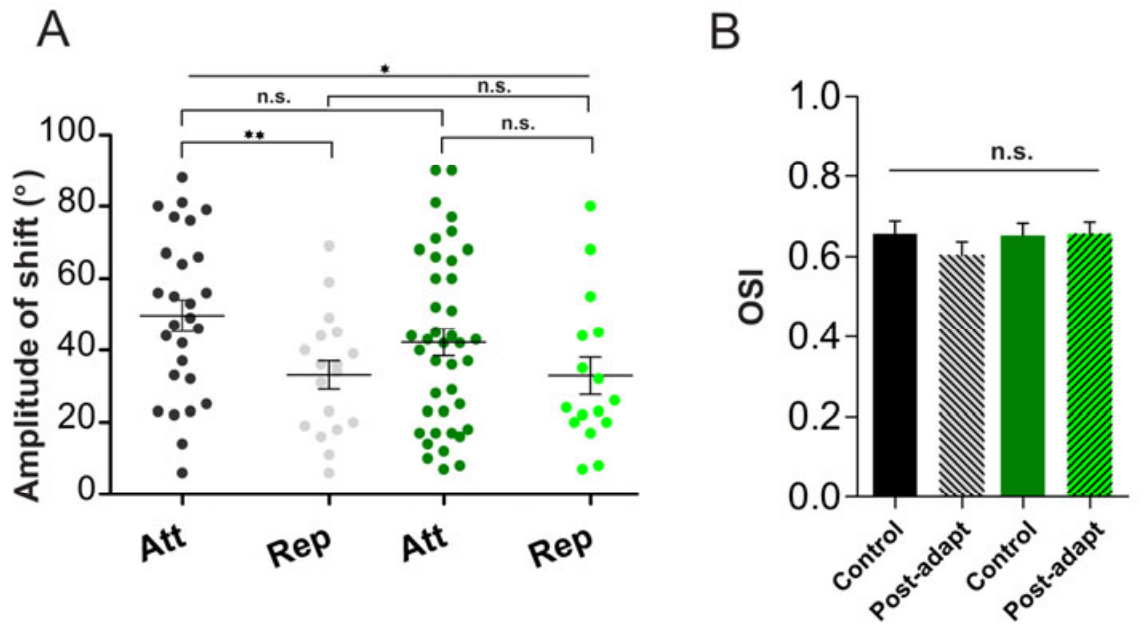


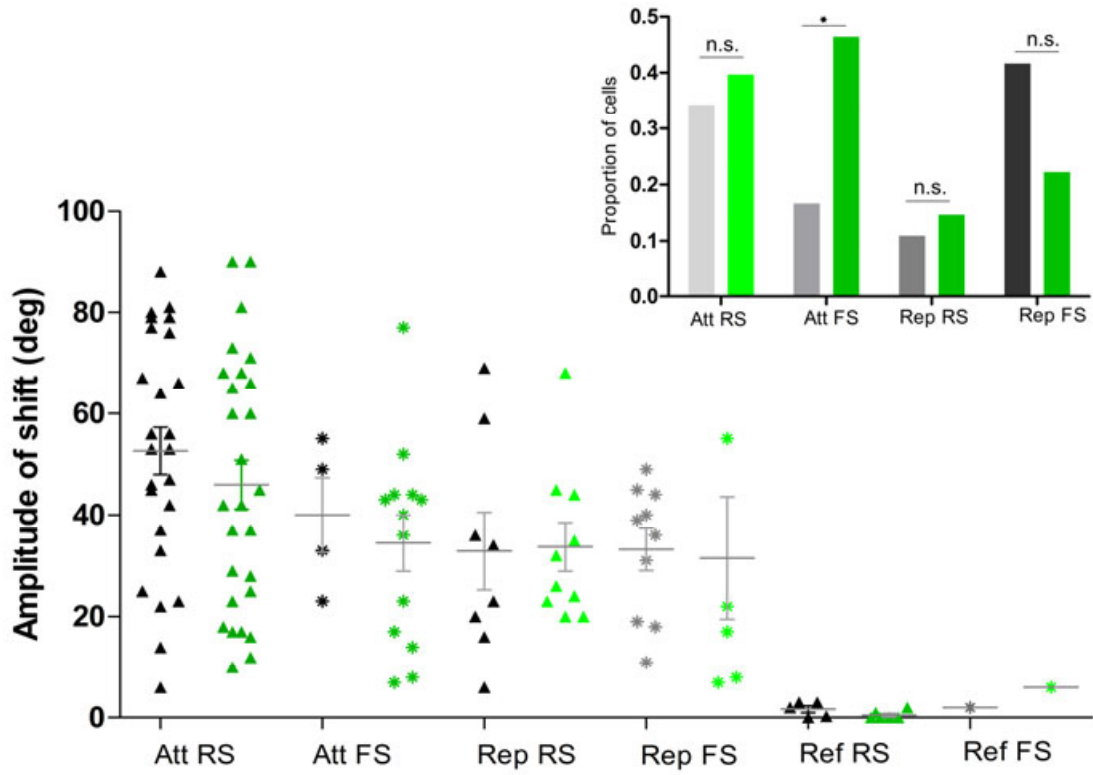
A Supragranular



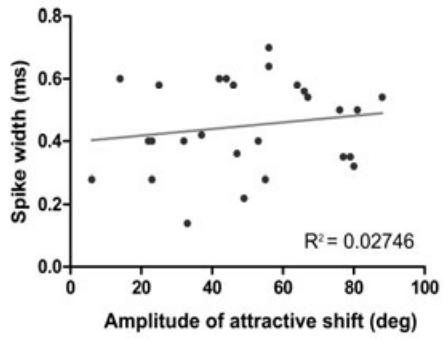
B Infragranular



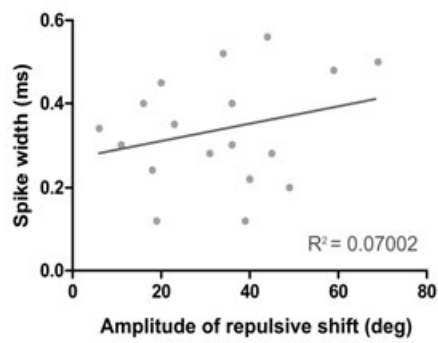




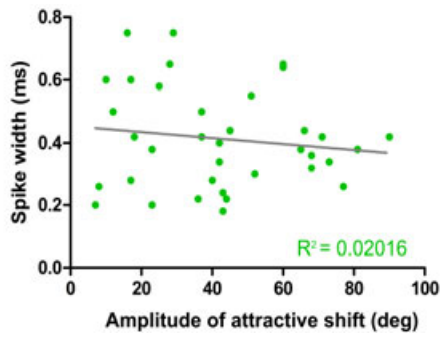
A



B



C



D

